Available online at www.sciencedirect.com

ScienceDirect

International Journal of Solids and Structures 44 (2007) 5742–5751

INTERNATIONAL JOURNAL OF SOLIDS AND STRUCTURES

www.elsevier.com/locate/ijsolstr

Polycrystalline kinematics: An extension of single crystal kinematics that incorporates initial microstructure

William A. Counts [a,*], Michael V. Braginsky [b], Corbett C. Battaile [b], Elizabeth A. Holm [b]

[a] *Max-Planck-Institute fur Eisenforshung, Max-Plank-Str. 1, 40237 Dusseldorf, Germany*

[b] *Computational Materials Science and Engineering Department, Sandia National Laboratories, P.O. Box 5800, Albuquerque, NM, 87185-1411, USA*

Received 8 March 2006; received in revised form 21 December 2006

Available online 30 January 2007

Abstract

Single crystal $\mathbf{F}^{\mathbf{e}}\mathbf{F}^{\mathbf{P}}$ kinematics are widely used as the basis for many crystal plasticity models. Within this kinematic framework, geometrically necessary dislocations (GNDs) initially do not exist and then they evolve as needed in the material. A shortcoming of this kinematic model is that there is no rigorous way to define the initial and evolving GND state in the same manner. By augmenting the single crystal $\mathbf{F}^{\mathbf{e}}\mathbf{F}^{\mathbf{P}}$ kinematics with a geometric argument, a consistent methodology for determining the initial and evolving GND state has been derived. The augmented kinematics describe GND related microstructural features in the undeformed material like low angle sub-grain boundaries and high angle grain boundaries. Therefore these kinematics are particularly applicable to polycrystalline materials.

Keywords: Crystal plasticity; Grain boundaries; Polycrystalline material; Kinematics; Geometrically necessary dislocations (GND)

1. Introduction

At the continuum level, the physical deformation of a material body can be expressed mathematically by the deformation gradient tensor, **F**. The mathematical definition of **F** at a material point depends only on the initial and current position of that material point. In order to embed some material physics in **F**, the total deformation gradient is decomposed into multiple components, where each component represents a different deformation mechanism or microstructural feature.

There are an infinite number of ways in which the deformation gradient can be decomposed. When modeling the elastic–plastic behavior of metallic materials, it is common to decompose **F** into two parts: one part that accounts for plastic deformation due to dislocation glide (plastic deformation gradient $\mathbf{F}^{\mathbf{P}}$), and one part

* Corresponding author. Tel.: +49 211 6792 312; fax: +49 211 6792 333.
E-mail address: w.counts@mpie.de (W.A. Counts).

0020-7683/$ - see front matter
doi:10.1016/j.ijsolstr.2007.01.027

that accounts for elastic stretching and rotation of the crystal lattice (elastic deformation gradient $\mathbf{F^e}$). Mathematically, it is possible to use an additive decomposition of $\mathbf{F}$ (Nemat-Nasser, 1979)

$$\mathbf{F} = \mathbf{F^e} + \mathbf{F^P} \tag{1}$$

However, there are criticisms in the literature on the physics of the additive elastic/plastic decomposition (Lee, 1981). Therefore, it is more common to employ a multiplicative decomposition (Bilby et al., 1955; Lee, 1969)

$$\mathbf{F} = \mathbf{F^e} \cdot \mathbf{F^P} \tag{2}$$

The complexity of the physical deformation process can lead to a large number of different deformation gradient decompositions. When the elastic rotation of the lattice dominates the elastic stretching of the lattice like during bulk forming processes, then the multiplicative decomposition in Eq. (2) can be simplified (Mathur and Dawson, 1989)

$$\mathbf{F} = \mathbf{R^e} \cdot \mathbf{F^P} \tag{3}$$

where $\mathbf{R^e}$ represents the elastic rotation deformation. On the other hand, when thermal effects are important like in thin polycrystalline films, the deformation gradient decomposition can be expanded to include these thermal effects (Yu et al., 1997)

$$\mathbf{F} = \mathbf{F}^{\theta} \cdot \mathbf{F^e} \cdot \mathbf{F^P} \tag{4}$$

where $\mathbf{F}^{\theta}$ is a thermal deformation gradient.

It is also possible to describe the geometrically necessary dislocation (GND) and damage state using the kinematics associated with $\mathbf{F}$. A number of different dislocation tensors that describe the GND within a material body have been proposed over the years. Some examples presented in Cermelli and Gurtin (2001) are the following:

$$(\operatorname{curl} \mathbf{F^e}) \cdot \mathbf{F^{e^{-T}}} \tag{5}$$

$$\operatorname{Curl} \mathbf{F^P} \tag{6}$$

$$\mathbf{R^{e^T}} \cdot (\operatorname{curl} \mathbf{F^{e^{-1}}}) \tag{7}$$

Note that there is no separate deformation gradient associated with GNDs in the above equations. Rather GNDs are routinely described within the elastic–plastic multiplicative decomposition (Eq. (2)). On the other hand, incorporating the effects of damage into $\mathbf{F}$ requires the additional terms. Bammann and Aifantis (1989) expanded the standard multiplicative decomposition to include a damage component

$$\mathbf{F} = \mathbf{F^e} \cdot \mathbf{F}^{v} \cdot \mathbf{F^P} \tag{8}$$

where $\mathbf{F^v}$ describes the permanent volume change due to a continuous distribution of voids. Clayton and McDowell (2003) proposed a hybrid additive-multiplicative decomposition approach to account for the effects of damage

$$\mathbf{F} = \mathbf{F^e} \cdot (\tilde{\mathbf{F}}^{m} + \tilde{\mathbf{F}}^{\mathbf{d}}) \tag{9}$$

where $\tilde{\mathbf{F}}^{m}$ is the residual matrix deformation gradient and $\tilde{\mathbf{F}}^{\mathbf{d}}$ represents the residual damage deformation gradient. Eq. (9) is not an additive elastic/plastic formulation. The additive decomposition applies only to damage.

While many of these formulations focus on modeling the evolving state of a material, it is also important that the kinematics describe the initial state as well. It is not realistic to assume that the initial state of a material is GND or damage free. For example, the GND state of polycrystalline metals is inhomogeneous due to the presence of grain boundaries and the microstructure of a single crystal is not homogeneous if low-angle boundaries are present. The GNDs and damage initially present will affect a material's response. Thus, it is important that kinematics are able to account for the initial as well as the evolving GND or damage state.

It is possible to describe the initial GND or damage state of the material body without using the kinematics described by $\mathbf{F}$. One such example is the work of Evers et al. (2004), where grain boundary dislocations make

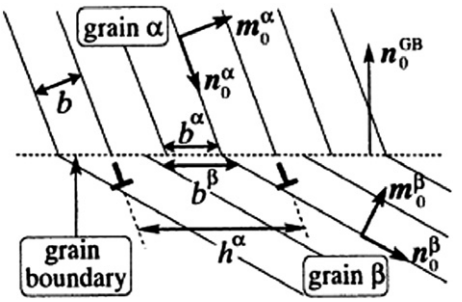

Fig. 1. Grain boundary dislocations as defined by Evers et al. (2004).

up the initial GND density. These grain boundary dislocations result from a lattice mismatch between two grains as shown in Fig. 1.

The initial GND density on each slip plane a $(\rho^{\alpha}{}_{\mathrm{GND}-0})$ was found by comparing the lengths of the burgers vectors in each grain, b^{α} and b^{β} in Fig. 1, according to

$$|\rho^{\alpha}_{\mathrm{GND}-0}| = \frac{1}{h^{\alpha 2}} = \left(\frac{1}{b^{\alpha}} - \frac{1}{b^{\beta}}\right)^2 \tag{10}$$

where h^{α} is the misfit length between the slip systems under consideration. There is certainly nothing wrong with initialization approaches that are not based on $\mathbf{F}$. However, kinematics should be able to describe the initial and evolving state of a material in a consistent manner.

In this paper, the $\mathbf{F} = \mathbf{F^e} \cdot \mathbf{F^P}$ kinematics are augmented with a geometric argument that introduces a natural configuration where the initial GND state can be defined. The augmented kinematics are then combined with well developed $\mathbf{F} = \mathbf{F^e} \cdot \mathbf{F^P}$ kinematics and termed polycrystalline kinematics. There are two dislocation tensors defined in the polycrystalline kinematics: one that describes the initial GND state, and one that describes the evolving GND state. Both of these dislocation tensors are determined in the same manner based on the work Cermelli and Gurtin (2001). Thus the polycrystalline kinematics provides a compete and consistent kinematical description for the deformation of a material body that has an initially non-zero GND state.

In the following discussion, a number of different kinematic configurations are presented, and the following notation is used throughout:

- Capital letters indicate a quantity in the reference configuration.
- Lower case letters indicate a quantity in the current configuration.
- A hat over a capital letter, $\hat{\mathrm{B}}$ for example, indicates a quantity in the intermediate configuration.
- A tilde over a capital letter, $\tilde{\mathrm{B}}$ for example, indicates a quantity in the natural configuration. (The natural configuration is defined in Section 3).
- An SC superscript, B^{SC} for example, indicates a quantity in the single crystal configuration. (The single crystal configuration is defined in Section 3).

This convention applies to indices as well. In addition, bold letters indicate vectors and tensors in symbolic notation. A dot over a quantity, $\dot{\mathrm{B}}$ for example, represents an ordinary time derivative. Repeated indices denotes summation over those indices. The inner product of two second-rank tensors is defined as $\mathbf{A} \cdot \mathbf{B} = \mathbf{C}$ where $C_{\mathrm{ik}} = A_{\mathrm{ij}} B_{\mathrm{jk}}$.

The curl operator used in this paper is not the standard definition used by Malvern (1969), but rather:

$$(\mathrm{Curl}\ \mathbf{T})_{\mathrm{IJ}} = \varepsilon_{\mathrm{IRS}} T_{\mathrm{JS,R}} \tag{11}$$

$$(\mathrm{curl}\ \mathbf{t})_{\mathrm{ij}} = \varepsilon_{\mathrm{irs}} t_{\mathrm{js,r}} \tag{12}$$

where $\varepsilon_{\mathrm{IJS}}$ and $\varepsilon_{\mathrm{ijs}}$ are the permutation symbol. In keeping with the notation convention described above, "Curl" refers to the curl operator with respect to the reference configuration, while "curl" refers to the curl operator with respect to the current configuration.

2. Single crystal kinematics

At the continuum level, the physical deformation of a material body can be expressed mathematically by the deformation gradient tensor, **F**. Bilby et al. (1955) and Lee (1969) proposed a model for single crystals in which the physical deformation represented by **F** is multiplicatively decomposed into an elastic deformation gradient, $\mathbf{F}^{\mathbf{e}}$, and a plastic deformation gradient, $\mathbf{F}^{\mathbf{P}}$, as

$$\mathbf{F} = \mathbf{F}^{\mathbf{e}} \cdot \mathbf{F}^{\mathbf{P}} \tag{13}$$

This deformation model decouples the elastic and plastic deformations resulting in the two-step deformation process shown in Fig. 2.

Within the deformation model, the lattice is first sheared plastically as a result of dislocation glide as described by $\mathbf{F}^{\mathbf{P}}$. This dislocation motion produces a shape change but no lattice orientation change. The shape change described by $\mathbf{F}^{\mathbf{P}}$ can produce voids and overlaps in the intermediate configuration resulting in an incompatible, non-physical configuration. Compatibility is then restored in the current configuration when the lattice is elastically stretched and rotated by $\mathbf{F}^{\mathbf{e}}$. Note: $\mathbf{F}^{\mathbf{e}}$ does not necessarily represent a reversible elastic deformation.

Mathematically, **F**, $\mathbf{F}^{\mathbf{e}}$, and $\mathbf{F}^{\mathbf{P}}$ are mappings between the three configurations shown in Fig. 2. By definition, each deformation gradient maps a differential line segment from one configuration to another via

$$\mathbf{F} \cdot d\mathbf{X} = d\mathbf{x} \quad d\mathbf{X} = \mathbf{F}^{-1} \cdot d\mathbf{x} \tag{14}$$

$$\mathbf{F}^{\mathbf{e}} \cdot d\hat{\mathbf{X}} = d\mathbf{x} \quad d\hat{\mathbf{X}} = \mathbf{F}^{\mathbf{e}^{-1}} \cdot d\mathbf{x} \tag{15}$$

$$\mathbf{F}^{\mathbf{P}} \cdot d\mathbf{X} = d\hat{\mathbf{X}} \quad d\mathbf{X} = \mathbf{F}^{\mathbf{P}^{-1}} \cdot d\hat{\mathbf{X}} \tag{16}$$

where $d\mathbf{X}$, $d\mathbf{x}$, and $d\hat{\mathbf{X}}$ are differential line segments in the reference, current, and intermediate configurations respectively. Because **F** describes the physical deformation, **F** must represent a smooth one-to-one mapping, or compatible deformation. A line integral with no closure failure, for a path enclosing an area, defines a compatible deformation and can be written as

$$\oint_{C} d\mathbf{x} = \oint_{c} \mathbf{F}\ d\mathbf{X} = \mathbf{0} \tag{17}$$

where c and C are paths in the current and reference configurations respectively. On the other hand, $\mathbf{F}^{\mathbf{e}}$ and $\mathbf{F}^{\mathbf{P}}$ individually are not required to represent compatible deformations. Except in the special cases when $\mathbf{F}^{\mathbf{e}}$ and $\mathbf{F}^{\mathbf{P}}$ are compatible (e.g., uniaxial, homogeneous deformation), there will be a net closure failure of a path enclosing an area. The line integral equations associated with the incompatible deformations described by $\mathbf{F}^{\mathbf{e}}$ and $\mathbf{F}^{\mathbf{P}}$, can be written as

$$\oint_{\hat{C}} d\hat{\mathbf{X}} = \oint_{c} \mathbf{F}^{\mathrm{e}^{-1}}\, d\mathbf{x} \neq \mathbf{0} \tag{18}$$

$$\oint_{\hat{C}} d\hat{\mathbf{X}} = \oint_{c} \mathbf{F}^{\mathrm{P}^{-1}}\, d\mathbf{x} \neq \mathbf{0} \tag{19}$$

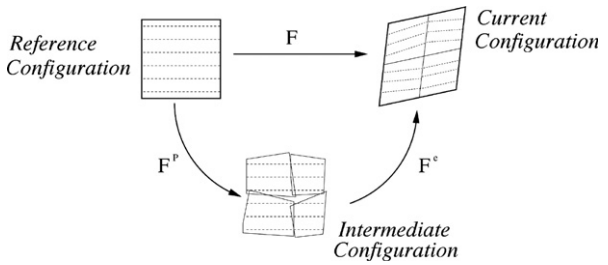

Fig. 2. Multiplicative decomposition of the deformation gradient.

where $\hat{C}$ is a path in the intermediate configuration. The line integrals and net closure failures in Eqs. (18) and (19) are identical to Burgers circuits and Burgers vectors used to quantify non-redundant dislocations, otherwise known as GNDs. This connection leads to a natural link between compatibility and microstructure.

Nye (1953) was one of the first to define a dislocation tensor that quantified GNDs within a continuum. Nye's geometric argument relating the Burgers vector, $\mathbf{b}$, to a general dislocation tensor, $\mathbf{g}$, may be expressed as

$$\mathbf{b} = \int_s \mathbf{g}\mathbf{n}\,da \tag{20}$$

where s is a surface and $\mathbf{n}$ is the normal to the surface s. An intermediate configuration dislocation tensor, $\hat{\mathbf{G}}$, can be derived from the compatibility equations for $\mathbf{F}^{\mathbf{e}}$ and $\mathbf{F}^{\mathbf{P}}$, Eqs. (18) and (19) using Stokes' theorem. Cermelli and Gurtin (2001) showed that the resulting dislocation tensor is

$$\hat{\mathbf{G}} = \frac{1}{J^{\mathbf{Fp}}}\mathbf{F}^{\mathbf{P}}\mathrm{Curl}\,\mathbf{F}^{\mathbf{P}} = J^{\mathbf{Fe}}\mathbf{F}^{\mathbf{e}^{-1}}\mathrm{curl}\,\mathbf{F}^{\mathbf{e}^{-1}} \tag{21}$$

where $J^{\mathbf{Fp}}$ is the determinant of $\mathbf{F}^{\mathbf{P}}$ and $J^{\mathbf{Fe}}$ is the determinant of $\mathbf{F}^{\mathbf{e}}$. In metals, plastic deformation is assumed to be isochoric meaning $J^{\mathbf{Fp}} = 1$. The dislocation tensor in Eq. (21) is one of many that have been proposed in the literature. Like the $\hat{\mathbf{G}}$ defined in Eq. (21), many of the proposed dislocation tensors are based on compatibility equations.[1] See Cermelli and Gurtin (2001) for a complete discussion on this topic.

It is straightforward and appropriate to apply the single crystal kinematics to a single crystal that has no initial GNDs (i.e., a single crystal that is homogeneous in orientation space). The initial conditions for such a case are the following:

$$\mathbf{F}^{\mathbf{e}}_{\mathbf{0}} = \mathbf{I}, \quad \mathbf{F}^{\mathbf{P}}_{\mathbf{0}} = \mathbf{I}, \quad \mathbf{F}_{\mathbf{0}} = \mathbf{I} \tag{22}$$

As a result of these initial conditions, no GNDs are initially present in the intermediate configuration because

$$\mathrm{Curl}\,\mathbf{F}_0 = \mathbf{0} \tag{23}$$

Problems with this formulation arise when GNDs are present in the initial material body that exists in the reference configuration. Examples of GND structures that could be present in the reference configuration are low angle boundaries in metal single crystals, and high angle boundaries in polycrystalline metals.

3. Single crystal kinematics applied to polycrystalline materials

Single crystal $\mathbf{F}^{\mathbf{e}}\mathbf{F}^{\mathbf{P}}$ kinematics are routinely applied to polycrystals (e.g., Mathur and Dawson, 1989; Kalidindi and Schoenfeld, 2000). In these models, a polycrystal is introduced into the reference configuration. The orientations of each grain ($\mathbf{R}^{\mathbf{e}}_{\mathbf{h}}$) in the polycrystal are initialized via

$$\mathbf{R}^{\mathbf{e}}_{\mathbf{h}} = \mathbf{R}\cdot\mathbf{R}^{\mathbf{Base}} \tag{24}$$

where $\mathbf{R}$ is a rotation and $\mathbf{R}^{\mathbf{Base}}$ is an initial state from which all the rotations in the $\mathbf{R}$ field are made. $\mathbf{R}^{\mathbf{Base}}$ can take any orientation value, but it is convenient to make $\mathbf{R}^{\mathbf{Base}} = \mathbf{I}$ making $\mathbf{R}^{\mathbf{e}}_{\mathbf{h}} = \mathbf{R}$. It is important to note that neither $\mathbf{R}$ nor $\mathbf{R}^{\mathbf{Grain}}$ represent a continuous field since each grain in the polycrystal has a different orientation.

It is possible to include Eq. (24) into the single crystal kinematics as shown in Fig. 3. A single crystal configuration has been added to the single crystal kinematics to represent the homogenous single crystal with an orientation $\mathbf{R}^{\mathbf{Base}}$. The term $\mathbf{F}_{\mathbf{h}}$ is introduced so that all mappings between configurations are done via deformation gradients. By the polar decomposition, $\mathbf{F}_{\mathbf{h}} = \mathbf{R}^{\mathbf{e}}_{\mathbf{h}}$ when the left and right stretch tensor ($\mathbf{V}^{\mathbf{e}}_{\mathbf{h}}$ and $\mathbf{U}^{\mathbf{e}}_{\mathbf{h}}$, respectively) equal the identity tensor.[2] In this context, $\mathbf{F}_{\mathbf{h}}$ does NOT represent a physical deformation (for that matter neither does $\mathbf{F}^{\mathbf{e}}$ or $\mathbf{F}^{\mathbf{P}}$) nor does $\mathbf{F}_{\mathbf{h}}$ account for processing or deformation history. $\mathbf{F}_{\mathbf{h}}$ is strictly a geometric argument needed to produce a polycrystalline material in the reference configuration.

[1] If compatibility is defined in terms of slip, then the dislocation tensor will depend on slip gradients (Fleck and Hutchinson, 1997).

[2] A further consequence of making $\mathbf{U}^{\mathbf{e}}_{\mathbf{h}} = \mathbf{V}^{\mathbf{e}}_{\mathbf{h}} = \mathbf{I}$ is that the reference configuration is stress-free.

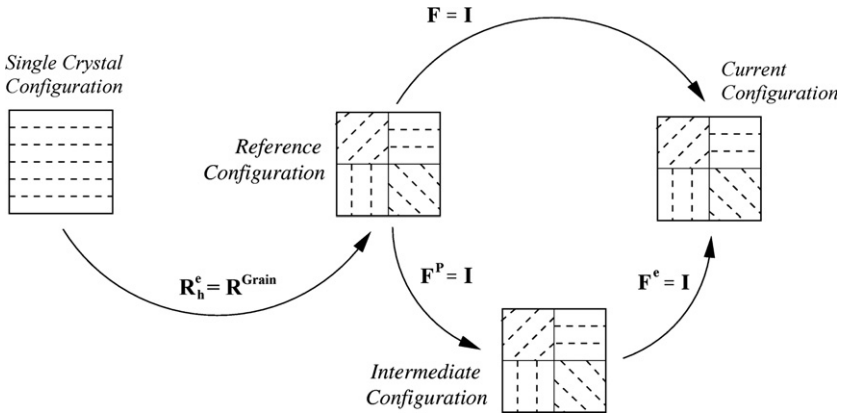

Fig. 3. Single crystal kinematics applied to a polycrystal at $t = 0$. Note that this figure is a schematic representation of polycrystalline deformation and therefore it does not contain any information about the scale of the kinematics. (The scale of the kinematic description is discussed in Section 5.)

The problem with this approach is that $\mathbf{F_h}$ must represent a compatible deformation. Mathematically, this means that

$$\text{Curl } \mathbf{F_h} = \text{Curl } \mathbf{R_h^e} = 0 \tag{25}$$

Enforcing this condition on an $\mathbf{F_h}$ or $\mathbf{R_h^e}$ field is not trivial. Physically, the lack of incompatibility between the single crystal configuration and the reference configuration means that no GNDs are present or are needed at the grain boundaries. Thus all the interfaces between grains are coherent boundaries, not an accurate description of grain boundaries.

4. Polycrystalline kinematics

In order to provide a kinematics framework that can define a GND state in the reference configuration, the geometric argument in Fig. 2 has been extended in this work. The grains in the reference configuration polycrystal are no longer described by just a rotation. Rather, the homogeneous material body in the single crystal configuration undergoes a total deformation ($\mathbf{F_h}$) to form the polycrystal in the reference configuration as shown in Fig. 4.

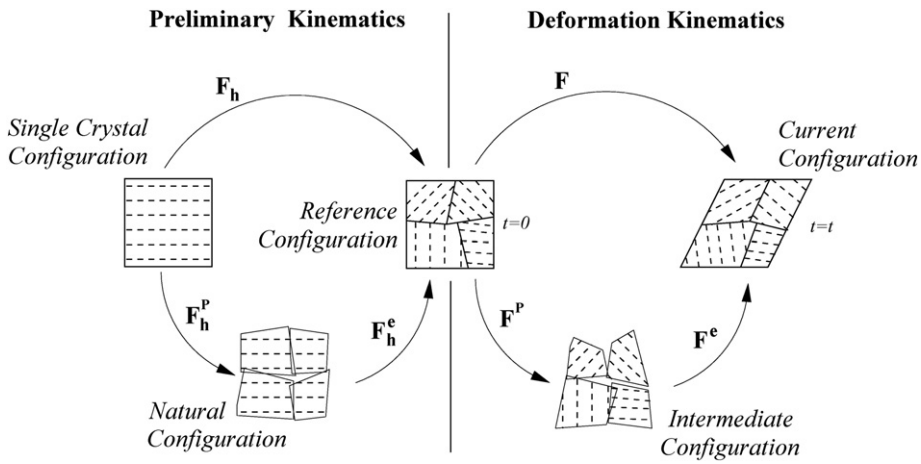

Fig. 4. Polycrystalline kinematics. Note that this figure is a schematic representation of polycrystalline deformation. The volumes shown in the natural and intermediate configurations should not imply that the scale of the kinematics is on the order of grain size. (The scale of the kinematics is discussed in Section 5.)

The purpose of the preliminary kinematics in Fig. 4 is to provide a framework by which the initial GND state can be determined in the same manner as the GND state in the intermediate configuration. With these kinematics, two separate dislocation tensors are defined: one in the natural configuration (representing the initial GND state) and one in the intermediate configuration (representing the evolving GND state). Note that this kinematic description is a construct, and is in no way intended to describe or represent any actual or prior material processing or other deformation history.

By augmenting rather than altering the single crystal kinematics to account for the initial GND state, the preliminary kinematics can be used with other decompositions of $\mathbf{F}$. For example, the preliminary kinematics could easily be incorporated into Yu's $\mathbf{F} = \mathbf{F}^{\boldsymbol{\theta}} \cdot \mathbf{F}^{\mathbf{e}} \cdot \mathbf{F}^{\mathbf{P}}$ model without altering the pre-existing kinematics that describe the evolving state of the material. In addition, the preliminary kinematics could be altered to describe damage, and therefore provide a consistent methodology by which the initial and evolving damage state is described. The flexibility and portability of the preliminary kinematics concept represents a major advantage of this approach.

4.1. General case

Within the expanded deformation model, $\mathbf{F_h}$ represents an effective deformation (not necessarily a physical deformation) that forms a polycrystal from a single crystal. $\mathbf{F_h}$ is multiplicatively decomposed into an elastic part, $\mathbf{F_h^e}$, and plastic part, $\mathbf{F_h^P}$, as follows

$$\mathbf{F_h} = \mathbf{F_h^e F_h^P} \tag{26}$$

By separating $\mathbf{F_h}$ in a similar fashion as $\mathbf{F}$, many of the same ideas and concepts associated with the single crystal kinematics can be applied to the preliminary kinematics. Just as before, the single crystal is initially deformed by $\mathbf{F_h^P}$, producing shape changes within the material but no orientation changes. The resulting shape changes create incompatibility in the form of voids and overlaps in the natural configuration as shown in Fig. 5.

$\mathbf{F_h^e}$ then restores compatibility in the reference configuration by elastically stretching and rotating the lattice planes.

By definition, $\mathbf{F_h}$, $\mathbf{F_h^e}$, and $\mathbf{F_h^P}$ map differential line segments from one configuration to another via

$$\mathbf{F_h} \cdot \mathrm{d}\mathbf{X}^{\mathbf{SC}} = \mathrm{d}\mathbf{X} \quad \mathrm{d}\mathbf{X}^{\mathbf{SC}} = \mathbf{F_h}^{-1} \cdot \mathrm{d}\mathbf{X} \tag{27}$$

$$\mathbf{F_h^e} \cdot \mathrm{d}\tilde{\mathbf{X}} = \mathrm{d}\mathbf{X} \quad \mathrm{d}\tilde{\mathbf{X}} = \mathbf{F_h^e}^{-1} \cdot \mathrm{d}\mathbf{X} \tag{28}$$

$$\mathbf{F_h^P} \cdot \mathrm{d}\mathbf{X}^{\mathbf{SC}} = \mathrm{d}\tilde{\mathbf{X}} \quad \mathrm{d}\mathbf{X}^{\mathbf{SC}} = \mathbf{F_h^P}^{-1} \cdot \mathrm{d}\tilde{\mathbf{X}} \tag{29}$$

where $\mathrm{d}\mathbf{X}^{\mathbf{SC}}$ and $\mathrm{d}\tilde{\mathbf{X}}$ are differential line segments in the single crystal and natural configurations respectively. Within the geometrical argument used to formulate the polycrystalline kinematics, $\mathbf{F_h}$ represents a compatible deformation. Thus, the compatibility equation associated with $\mathbf{F_h}$ can be written as

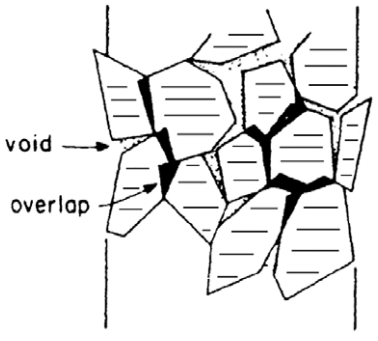

Fig. 5. An incompatible crystal in the natural configuration.

$$\oint_{C} d\mathbf{X} = \oint_{C^{SC}} \mathbf{F_h} \cdot d\mathbf{X}^{SC} = \mathbf{0} \tag{30}$$

where C^{SC} is a path in the single crystal configurations. Eq. (30) represents one the key points in the polycrystalline kinematics: the compatibility of the reference configuration is ensured by $\mathbf{F_h}$ not by $\mathbf{R_h^e}$ since

$$\text{Curl } \mathbf{F_h} = \mathbf{0}$$
$$\text{Curl } \mathbf{R_h^e} \neq \mathbf{0}.$$

Thus any $\mathbf{R_h^e}$ field is admissible to describe the orientations of the grains within the polycrystal in the reference configuration.

On the other hand, $\mathbf{F_h^e}$ and $\mathbf{F_h^P}$ are not required to represent compatible deformations and in general there is a closure failure associated with compatibility equations for $\mathbf{F_h^e}$ and $\mathbf{F_h^P}$

$$\oint_{\tilde{C}} d\tilde{\mathbf{X}} = \oint_{c} \mathbf{F_h^{e^{-1}}} \cdot d\mathbf{X} \neq \mathbf{0} \tag{31}$$

$$\oint_{\tilde{C}} d\tilde{\mathbf{X}} = \oint_{c} \mathbf{F}_h^{\mathbf{P}} \cdot d\mathbf{X}^{SC} \neq \mathbf{0} \tag{32}$$

where $\tilde{C}$ is a path in the natural configuration. By applying the $\mathbf{F^eF^P}$ dislocation tensor concepts derived by Cermelli and Gurtin (2001) to $\mathbf{F_h^e}$, and $\mathbf{F_h^P}$, a dislocation tensor in the natural configuration ($\tilde{\mathbf{G}}$) that describes the initial GND state can be defined as

$$\tilde{\mathbf{G}} = \frac{1}{J^{\mathbf{F_h^P}}} \mathbf{F_h^P} \cdot \text{Curl } \mathbf{F_h^P} = J^{\mathbf{F_h^{e^{-1}}}} \mathbf{F_h^{e^{-1}}} \cdot \text{Curl } \mathbf{F_h^{e^{-1}}} \tag{33}$$

where $J^{\mathbf{F_h^P}}$ is the determinant of $\mathbf{F_h^P}$ and $J^{\mathbf{F_h^P}}$ is the determinant of $\mathbf{F_h^e}$. Eq. (33) represents the most general form of the dislocation tensor in the natural configuration.

$\tilde{\mathbf{G}}$ was derived based on a geometric argument, and all the geometric information is contained within $\mathbf{F_h^e}$. Thus $\tilde{\mathbf{G}}$ further simplifies to

$$\tilde{\mathbf{G}} = J^{\mathbf{F_h^{e^{-1}}}} \mathbf{F_h^{e^{-1}}} \cdot \text{Curl } \mathbf{F_h^{e^{-1}}} \tag{34}$$

In this context there is no need to precisely define either $\mathbf{F_h^P}$ or $\mathbf{F_h}$. They are necessary in this model simply to ensure that the reference configuration is compatible.

The second dislocation tensor, $\hat{\mathbf{G}}$, describes the evolving dislocation state and is defined in the intermediate configuration. The form of this dislocation tensor is unchanged from the dislocation tensor described in the single crystal kinematics section, specifically Eq. (21). The total GND state, $\hat{\mathbf{G}}^{\mathbf{Tot}}$, is defined as the sum of $\tilde{\mathbf{G}}$, moved from the natural configuration to the intermediate configuration, and $\hat{\mathbf{G}}$:

$$\hat{\mathbf{G}}^{\mathbf{Tot}} = \mathbf{F^P} \cdot \mathbf{F_h^e} \cdot \tilde{\mathbf{G}} \cdot (\mathbf{F_h^e})^{-1} \cdot (\mathbf{F^P})^{-1} + \hat{\mathbf{G}} \tag{35}$$

where $\tilde{\mathbf{G}}$ is then pushed forward to the intermediate configuration using $\mathbf{R_h^e}$ (to move from the natural to the reference configuration) and $\mathbf{F^P}$ (to move from the reference to the intermediate configuration). A comparison of the single crystal kinematics and the polycrystalline kinematics is contained in Table 1.

Table 1
Summary of single and polycrystalline kinematics

Single crystal kinematics
Dislocation tensor: $\hat{\mathbf{G}} = \frac{1}{J^{\mathbf{F^P}}} \mathbf{F^P} \text{Curl } \mathbf{F^P} = J^{\mathbf{F^e}} \mathbf{F^{e^{-1}}} \text{curl } \mathbf{F^{e^{-1}}}$
Compatibility of the current configuration: $\text{Curl } \mathbf{F} = \mathbf{0}$
Polycrystalline kinematics
Dislocation tensor: $\tilde{\mathbf{G}} = \frac{1}{J^{\mathbf{F_h^P}}} \mathbf{F_h^P} \cdot \text{Curl } \mathbf{F_h^P} = J^{\mathbf{F_h^{e^{-1}}}} \mathbf{F_h^{e^{-1}}} \cdot \text{Curl } \mathbf{F_h^{e^{-1}}}$
$\hat{\mathbf{G}} = \frac{1}{J^{\mathbf{F^P}}} \mathbf{F^P} \text{Curl } \mathbf{F^P} = J^{\mathbf{F^e}} \mathbf{F^{e^{-1}}} \text{curl } \mathbf{F^{e^{-1}}}$
$\hat{\mathbf{G}}^{\mathbf{Tot}} = \mathbf{F^P} \cdot \mathbf{F_h^e} \cdot \tilde{\mathbf{G}} \cdot (\mathbf{F_h^e})^{-1} \cdot (\mathbf{F^P})^{-1} + \hat{\mathbf{G}}$
Compatibility of the reference configuration: $\text{Curl } \mathbf{F_h} = \mathbf{0}$
Compatibility of the current configuration: $\text{Curl } \mathbf{F} = \mathbf{0}$

4.2. An orientation dependent $\tilde{\mathbf{G}}$

Defining a $\mathbf{F}_{\mathbf{h}}^{\mathbf{e}}$ for Eqs. (33) and (34) that is physically meaningful is not straightforward. Since $\mathbf{F}_{\mathbf{h}}^{\mathbf{e}} = \mathbf{R}_{\mathbf{h}}^{\mathbf{e}} \cdot \mathbf{U}_{\mathbf{h}}^{\mathbf{e}}$, $\mathbf{F}_{\mathbf{h}}^{\mathbf{e}}$ contains information about both the stretching ($\mathbf{U}_{\mathbf{h}}^{\mathbf{e}}$) and the rotation of the lattice planes ($\mathbf{R}_{\mathbf{h}}^{\mathbf{e}}$). If it is assumed that the polycrystal in the reference configuration is stress-free everywhere (no internal stress state), then $\mathbf{U}_{\mathbf{h}}^{\mathbf{e}} = \mathbf{I}$ and $\mathbf{F}_{\mathbf{h}}^{\mathbf{e}} = \mathbf{R}_{\mathbf{h}}^{\mathbf{e}}$. The resulting $\tilde{\mathbf{G}}$ tensor then only depends on grain orientations via

$$\tilde{\mathbf{G}} = \mathbf{R}_{\mathbf{h}}^{\mathbf{e}^{-1}} \cdot \operatorname{Curl} \mathbf{R}_{\mathbf{h}}^{\mathbf{e}^{-1}} \tag{36}$$

where $J^{\mathbf{R}_{\mathbf{e}}^{\mathbf{h}}} = 1$. Note that the assumption of a stress free reference configuration used to derive Eq. (36) is a constitutive assumption. In reality, there are internal stresses present in an undeformed material. Accounting for internal stresses at the continuum level remains a challenge.

5. Kinematic scales

In the single crystal kinematics, the statistical volume element (SVE)[3] that characterizes $\hat{\mathbf{G}}$ is defined by the size of the burgers circuit (i.e., c, C, and $\hat{\mathbf{C}}$ in Eqs. (11)–(13). It is important that the size of the burgers circuit is appropriately sized. If the SVE is too small, for example on the order of dislocation spacing, then every dislocation in the material becomes a GND. If the SVE is too large, for example on the order of specimen dimensions, then the GND content within the single crystal approaches 0. Generally, the GND structures described by $\hat{\mathbf{G}}$ are at the microscale. Thus $\hat{\mathbf{G}}$ is also a microscale quantity.

Within the polycrystalline kinematics, the SVE associated with $\tilde{\mathbf{G}}$ and $\hat{\mathbf{G}}$ must be the same, otherwise it is not possible to add them together to get $\hat{\mathbf{G}}^{\mathbf{Tot}}$ in Eq. (35). In order to resolve the primary feature of interest, grain boundaries, the SVE associated with all the dislocation tensors ($\tilde{\mathbf{G}}$, $\hat{\mathbf{G}}$, and $\hat{\mathbf{G}}^{\mathbf{Tot}}$) must be sufficiently large so that the GND state vanishes far from the grain boundary and but not so large that it contains more than one grain. Such an SVE would be on the order of sub-grain size making the GND state described by $\hat{\mathbf{G}}^{\mathbf{Tot}}$ a micro-scale quantity.

6. Limitations of the polycrystalline kinematics

In the single crystal kinematics, the $\hat{\mathbf{G}}$ tensor represents the evolving GND state within a single crystal due to an applied deformation. The GND arrays represented by $\hat{\mathbf{G}}$ are typically low angle boundaries (boundaries with a misorientation less than 10°–15°. Because it is appropriate to describe low angle boundaries as arrays of GNDs, it is appropriate to represent the GND structures described by the single crystal kinematics with $\hat{\mathbf{G}}$.

In the polycrystalline kinematics, $\tilde{\mathbf{G}}$ represents the GND state at grain boundaries. In this context, $\tilde{\mathbf{G}}$ can be applied to a range of different grain boundaries: low angle boundaries, high angle boundaries, and special (or low energy) boundaries. As stated previously, it is possible to describe a low angle boundary as dislocation array of GNDs. However, characterizing high angle and special boundaries solely as GND arrays may not be ideal. Despite this shortcoming, the kinematics approach that defines $\hat{\mathbf{G}}^{\mathbf{Tot}}$ is an important first step towards describing grain boundaries and other dislocation arrays that exist in a material body in the reference configuration.

7. Conclusions

The polycrystalline kinematics developed in this paper represent a kinematically consistent method in which microstructure (specifically GNDs) can be introduced into the reference configuration. The traditional $\mathbf{F} = \mathbf{F}^{\mathbf{e}} \cdot \mathbf{F}^{\mathbf{P}}$ kinematics are augmented with a geometric argument called the preliminary kinematics. In the preliminary kinematics, the natural configuration is defined and here the initial GND state is also defined. Because the preliminary kinematics are defined in a similar fashion as the $\mathbf{F} = \mathbf{F}^{\mathbf{e}} \cdot \mathbf{F}^{\mathbf{P}}$ kinematics, many of

[3] An SVE rather than RVE (representative volume element) is used here because statistical homogeneity within the volume element it is not a proiri assumed (Clayton and McDowell, 2003).

the same ideas and concepts associated with the single crystal kinematics are applied to the preliminary kinematics. Thus, the dislocation tensor in the natural configuration (representing the initial GND state) is defined in the same manner as the dislocation tensor in the intermediate configuration (representing the evolving GND state). By making the assumption that the reference configuration is stress-free, an initial dislocation tensor that depends only on orientations is derived.

Acknowledgements

The authors gratefully acknowledge Dr. David McDowell and Dr. Douglas Bammann for their helpful discussions. All work was performed at Sandia National Laboratories in Albuquerque, NM. Sandia is a multiprogram laboratory operated by Sandia Corporation, a Lockheed Martin Company, for the United States Department of Energy, under Contract No. DE-AC04-94AL85000.

References

Bammann, D.J., Aifantis, E.C., 1989. A damage model for ductile metals. Nuclear Engineering and Design 116, 355–362.

Bilby, B.A., Bullough, R., Smith, E., 1955. Continuous distributions of dislocations: a new application of methods of non-riemannian geometry. Proceedings of the Royal Society of London Series A – Mathematical and Physical Sciences 231, 263–273.

Cermelli, P., Gurtin, M.E., 2001. On the characterization of geometrically necessary dislocations in finite plasticity. Journal of Mechanics and Physics of Solids 49, 1539–1568.

Clayton, J.D., McDowell, D.L., 2003. Finite polycrystalline elastoplasticity and damage: multiscale kinematics. International Journal of Solids and Structures 40, 5669–5688.

Evers, L.P., Brekelmans, W.A.M., Geers, M.G.D., 2004. Scale dependent crystal plasticity framework with dislocation density and grain boundary effects. International Journal of Solids and Structures 41, 5209–5230.

Fleck, N.A., Hutchinson, J.W., 1997. Strain gradient plasticity. Advances in Applied Mechanics 33, 295–361.

Kalidindi, S.R., Schoenfeld, S.E., 2000. On the prediction of yield surfaces by the crystal plasticity models for polycrystals. Materials Science and Engineering A239, 120–129.

Lee, E.H., 1969. Elastic–plastic deformation at finite strains. ASME Journal of Applied Mechanics 36, 1–6.

Lee, E.H., 1981. Some comments on elastic–plastic analysis. International Journal of Solids and Structures 17, 859–872.

Malvern, L.E., 1969. Introduction to the Mechanics of a Continuum Media. Prentice-Hall.

Mathur, K.K., Dawson, P.R., 1989. On modeling the development of crystallographic texture in bulk forming processes. International Journal of Plasticity 5, 67–94.

Nemat-Nasser, S., 1979. Decomposition of strain measures and their rates in finite deformation elastoplasticity. International Journal of Solids and Structures 15, 155–166.

Nye, J.F., 1953. Some geometrical relations in dislocated crystals. Acta Metallurgica 1, 153–162.

Yu, J., Maniatty, A.M., Knorr, D.B., 1997. Model for predicting thermal stresses in thin polycrystalline films. Journal of the Mechanics and Physics of Solids 45, 511–534.